Local isotropy and geometry of particle flux lines in diffusion-limited aggregation

1996 J. Phys. A: Math. Gen. 29 1785

(http://iopscience.iop.org/0305-4470/29/8/025)

J. Phys. A: Math. Gen. **29** (1996) 1785–1794. Printed in the UK

Local isotropy and geometry of particle flux lines in diffusion-limited aggregation

Chi-Hang Lam

Department of Applied Physics, Hong Kong Polytechnic University, Hung Hom, Hong Kong

Received 12 October 1995, in final form 3 January 1996

Abstract. We present a theoretical description of the branch orientation and the geometry of walker flux lines in diffusion limited aggregation (DLA). It is based on the self-similarity and non-directedness of the branch structure and explains recent numerical results on the probability distribution of the branch orientation and the angle of particle attachment. Our results support the idea that asymptotically large off-lattice DLA clusters are locally isotropic and every individual walker flux line exhibits a certain type of self-similarity.

1. Introduction

The diffusion-limited aggregation (DLA) [1] is one of the most important stochastic fractal growth models [2]. Despite intensive study, few analytical results exist. In this paper, we suggest a convolution equation describing the branch orientation and the geometry of the walker flux lines in DLA. It explains recent numerical findings on the probability distribution of the angle of attachment of the walkers [3]. This work focuses on off-lattice DLA.

Witten and Sander [1] first proposed that the geometry of DLA is scale invariant. The two-point density–density correlation function falls off with distance in the form of a power law for length scales between that of the cluster and the constituent particles. However, Meakin and Viscek [4] subsequently found that the density correlation is anisotropic even for off-lattice DLA. When grown in the radial geometry, the tangential correlation decays algebraically with an exponent $\alpha_\perp \simeq 0.41$, which is different from the radial exponent $\alpha_\parallel \simeq 0.29$. They also concluded from their extrapolation that the difference in the exponents is not due to finite-size effects. As a result, there had been a general belief that DLA is self-affine.

However, the self-affine hypothesis of DLA does not seem to be intuitively satisfactory. If we assume self-affinity, anisotropically magnified segments of DLA should be statistically similar to other larger segments. We may naturally expect that the particle flux lines and the equipotential lines for the magnified segments can be obtained by the same anisotropic rescaling. This is because those lines are critical in the growth process and it is hard to believe that do not conform to scalings similar to that of the cluster. However, this results in flux lines crossing the equipotential lines at angles other than 90° since anisotropic magnification is not an orthogonal transformation, and this is impossible.

Besides the correlation functions, the branch orientation can also characterize the anisotropy of DLA. Mandelbrot and Vicsek [9] constructed a directed recursive fractal model for diffusion-limited deposition in which all branches at every level subtend acute angles with the upward vertical direction. Their model illustrates how a fractal can have anisotropic

0305-4470/96/081785+10$19.50

density correlation, although it can be shown that the exponents for the power-law decay of the correlation function remain isotropic. In contrast, we suggest that the branch structure of DLA is non-directed. After many levels of side-branching, the side branches point in all directions. Asymptotically large DLA clusters are locally isotropic. The situation is similar to the case of the Koch curve.

The rest of the paper is organized as follows. Section 2 summarizes recent numerical results on the branch orientation and the angle of attachment for DLA. Section 3 derives properties of the Koch curve which can be associated with the numerical results for the branch orientation of DLA. In section 4, numerical results on the probability distribution of the angle of attachment are explained using a convolution equation. Section 5 suggests plausible realizations of the equation which give physically acceptable results. Section 6 discusses a related self-similarity of the walker flux lines. We conclude with some further discussions in section 7.

2. Recent numerical results on local isotropy

One way to test the isotropy, motivated by Mandelbrot and Vicsek's directed recursive model of DLA [9], is to measure the probability distribution $P(\phi)$ of the branch orientation angle, ϕ, which is the angle subtended between the direction of a branch and the outward local radial direction. The numerical measurements on the branch orientation angle were carried out by Lam *et al* [3]. They adopted the Horton–Strahler scheme of branch definition and ordering. The branch orientation angle ϕ is measured counterclockwise from the position vector pointing from the centre of the cluster to the base of the branch to the branch-orientation vector pointing from the base to the tip of the branch [3]. If a branch points radially outward, inward, or tangentially, we have respectively $\phi \simeq 0, \pm\pi$ or $\pm\pi/2$, respectively. The directed recursive model predicts that at all levels of side-branching, the proportion of the forward pointing branches is more than that of the backward ones. Alternatively, the local isotropy of DLA requires that the proportions should be equal asymptotically and $P(\phi)$ should approach a constant function for high-order side branches.

Lam *et al* computed the distribution $P(\phi)$ for various branch orders [3]. They found that while the low-order main stems point radially outward, the high-order side branches follow much more isotropic distributions. There is a clear trend that $P(\phi)$ tends to the uniform distribution as the branch order increases. Another interesting observation is that the distributions for the highest branch orders investigated fit well to cosine functions of small amplitudes in the form:

$$P(\phi) = \frac{1}{2\pi} + a\cos(\phi)\,. \tag{1}$$

We will suggest an explanation for this observation in section 3.

A related approach to investigate the isotropy is to measure the probability distribution of the angle of particle attachment θ. This angle was also studied by Hegger and Grassberger [6]. Our discussions will concentrate on Lam *et al*'s results [3] which contain analysis relevant to the present work. During the growth of DLA, a sticking event occurs when a new random walker joins the cluster. The particle in the cluster which the walker adheres to is called the parent of the new particle. The attachment direction points from the centre of the parent to that of the new particle. The angle of attachment θ is defined as the angle subtended from the attachment direction to the outward radial direction which points from the centre of the cluster to that of the parent. Similarly to the case of the branch-orientation angle, forward, backward or tangential attachments correspond, respectively, to

$\theta \simeq 0, \pm\pi$ or $\pm\pi/2$. Let $P(\theta, N)$ be the probability distribution of θ as a function of the cluster size N. The numerical result of $P(\theta, N)$ [3] also shows a clear trend towards the uniform distribution as N increases. In addition, from the cosine expansion:

$$P(\theta, N) = \frac{1}{2\pi} + \sum_{n=1}^{\infty} a_n(N)\ \cos(n\theta) \tag{2}$$

it was found that the coefficients fall off in simple algebraic forms for $N \gtrsim 300$:

$$a_n(N) \simeq A_n N^{-\gamma_n} \tag{3}$$

for $n = 1$ and 2, where $\gamma_1 = 0.0997(3)$, $A_1 = 0.309(2)$, $\gamma_2 = 0.67(3)$ and $A_2 = 1.2(3)$. The bracketed values are the fitting errors. However, for $n \geqslant 3$, the $a_n(N)$'s are too small to be measured. For the largest value of $N = 614\,400$ investigated, the lowest harmonic dominates so overwhelmingly that $P(\theta, N)$ has converged to the cosine distribution:

$$P(\theta, N) = 1/2\pi + a_1(N)\cos(\theta) \tag{4}$$

within their numerical errors. Extrapolation of (3) and (4) shows that asymptotically the distribution approaches the constant function corresponding to locally isotropic attachment process. We will present a possible explanation for equations (3) and (4) in section 4.

3. Branch orientation: analogy with the Koch curve

The cosine distributions for both the branch orientation and the angle of attachment in (1) and (4) are rather rare cases in which any properties of DLA fit nicely to simple non-trivial functional forms. We suggest that they result from the non-directed branch structure. We now derive an analogous discrete cosine distribution for the segment orientations of the Koch curve, which is also non-directed. We suggest that similar arguments also describe the branch orientation of DLA.

For the Koch curve, a segment can only take one of the six orientations corresponding to $0, \pi/3, \ldots 5\pi/3$. The probability distribution of the orientation can be specified simply by a column vector $\boldsymbol{P}$ with six elements. The nth element ($n = 0$ to 5) of $\boldsymbol{P}$ specifies the fraction of the segments with orientation $n\pi/3$. Let us start with an upward facing generator corresponding to a 0 orientation angle. At this initial stage, the distribution is $\boldsymbol{P}_1 = (1, 0, 0, 0, 0, 0)^t$. For the second generation with four segments, two of them keep the same orientation while the other two are rotated by $\pm\pi/3$. Therefore, $\boldsymbol{P}_2 = (\frac{1}{2}, \frac{1}{4}, 0, 0, 0, \frac{1}{4})^t$. In general, for each increment in the number of generations, every segment splits into four and two of them are rotated by $\pi/3$ in either direction irrespective to any fixed reference direction or history of splitting. Therefore, the distribution $\boldsymbol{P}_{l+1}$ for the $(l+1)$th generation pre-fractal relates to $\boldsymbol{P}_l$ linearly in the form

$$\boldsymbol{P}_{l+1} = \boldsymbol{A}\boldsymbol{P}_l \tag{5}$$

where A is the tridiagonal matrix:

$$\boldsymbol{A} = \tfrac{1}{4}\begin{pmatrix} 2 & 1 & 0 & 0 & 0 & 1 \\ 1 & 2 & 1 & 0 & 0 & 0 \\ 0 & 1 & 2 & 1 & 0 & 0 \\ 0 & 0 & 1 & 2 & 1 & 0 \\ 0 & 0 & 0 & 1 & 2 & 1 \\ 1 & 0 & 0 & 0 & 1 & 2 \end{pmatrix}. \tag{6}$$

The evolution from $\boldsymbol{P}_l$ to $\boldsymbol{P}_{l+1}$ is mathematically equivalent to a discrete random walk on a ring with six sites. The normal modes are the harmonics. For large l, the lowest harmonic dominates and the distribution converges to

$$[\boldsymbol{P}_l]_n = \frac{1}{6} + \frac{1}{\sqrt{3}}\left(\frac{3}{4}\right)^l \cos\left(\frac{n\pi}{3}\right) \tag{7}$$

where $[\boldsymbol{P}_l]_n$ denotes the nth element of $\boldsymbol{P}_l$. Therefore, for sufficiently high generations, the distribution of the segment orientation is approximately a discrete cosine. In addition, the amplitude of the cosine term decreases exponentially with respect to the number of generations l and the distribution converges to the uniform one asymptotically.

As a result, both the distributions of the branch orientation for DLA and that of the segment orientation for the Koch curve in (1) and (7), respectively, are cosines. This does not seem to be a coincidence and we aware of no alternative explanation for (1). We suggest that DLA is non-directed similarly to the Koch curve and the above derivation of the cosine distribution for the Koch curve can be applied to give (1).

The cosine distribution is a consequence of the history-independent rotations of the segments as the number of generations increases. The angle of rotation is $\pm\pi/3$. For DLA, analogous angle of rotation is the angle subtended between a side branch and its parent branch and is a stochastic variable. Adopting a variant of the Horton–Strahler branch ordering scheme, Ossadnik [7] found numerically that for very large clusters the average branch subtending angle is about $\pm 38^\circ$. For DLA, the distribution $P(\phi)$ is a continuous function and (5) has to be replaced by a convolution equation. Although the quantitative form of the propagator, which is analogous to the matrix $\boldsymbol{A}$ in (6), is unknown, important features of the solution including the cosine distribution (1) at high branch orders can similarly be derived.

Equation (7) predicts that the amplitude of the cosine distribution decreases exponentially with respect to the number of generations l. However, the numerical value of the corresponding amplitude of the cosine distribution for the branch orientation angle does not decrease exponentially with the branch order [3]. This is possibly due to finite-size effects resulting from considerable short range history dependence in the branching process. In fact, the radial main stems physically forbid some of the higher order branches to lie radially. This exclusion is also the cause of the noticeable dip in the distribution of $P(\phi)$ around $\phi = 0$ for the low-order branches [3]. The dip disappears at higher orders indicating that the history dependence only extends up to a small number of orders. We expect that using sufficiently large clusters, the exponential decay of the amplitude with respect to the branch order can be observed numerically.

4. Angle of attachment

The interesting numerical results on the distribution of the angle of attachment obtained by Lam *et al* [3] in (2) and (3) can be derived similarly by assuming the non-directed branch structure of DLA. Our discussions will be based on the following picture of DLA growth. To add a particle to the cluster, the Laplacian potential is solved to obtain the walker flux lines. A new particle is initially positioned randomly with uniform probability on a big circle centred at the seed of the cluster. It subsequently traces the flux line deterministically towards the cluster until it hits and becomes part of it. The direction of the attachment is thus tangential to the flux line at the point of contact. This approach is mathematically equivalent to the random walker method. Figure 1 shows 200 flux lines with uniformly spaced starting positions. They are all equally likely representations of the next growth

step. We will concentrate on the statistical nature of the geometry of these flux lines. Our arguments can also be adapted to describe the field lines for the Laplacian potential around the Koch curve.

Since the details of the cluster have little influence on the potential far away, starting from infinity a flux line extends radially inward until it is close enough to be affected by the geometry of the a main branch. At this stage, the geometry of the side branches is unimportant. Depending on the position of the flux line relative to the nearest main branch, it either keeps approaching the branch radially or turns to approach the branch from one of the sides. After extending further towards the cluster, the geometry of the nearest side branch becomes important. Again, the flux line extends either towards the tip or turns to one of the sides of the closest side branch. Similar situations recur for higher and higher order side branches until the geometry of the constituent particles becomes relevant.

If a flux line is perfectly straight pointing radially from infinity to the cluster, the corresponding angle of attachment θ is 0 according to Lam *et al*'s definition [3] summarized in section 2. In general, every flux line curves and it can be shown that θ is approximately the sum of all the turns along the whole curve, apart from an unimportant additive term. From the above simple picture that a flux line turns whenever it is affected by a further level of side-branching, the total number of turns in a flux line is related to the total number of levels of side-branching it encounters. Since this is a stochastic variable, we consider the average over all the flux lines weighted by their probability. As a result, the average number of turns in a flux line is proportional to the average number of branch levels the line encounters, which is in turn proportional to the total number of branch levels in the whole cluster. In the radial geometry, the number of branch levels is proportional to $\tau = \ln N$ [8, 7]. Therefore, there will be on average an additional turn on a flux line whenever τ increases by a constant amount denoted by $\Delta\tau$ or the cluster size N increases by a constant factor $\exp(\Delta\tau)$. Let $\Delta\theta$ be the additional turn for a particular flux line. The corresponding angle of attachment, which could have been, say, θ' without the additional turn, now becomes $\theta = \theta' + \Delta\theta$. Let us reparametrize the distribution $P(\theta, N)$ to $P(\theta, \tau)$. Assuming that the turns in every flux line are uncorrelated or history-independent, due to the additional turn caused by an increase in the cluster size, $P(\theta, \tau)$ evolves according to the convolution equation:

$$P(\theta, \tau + \Delta\tau) = \int_{-\pi}^{\pi} G(\theta - \theta', \Delta\tau) P(\theta', \tau)\, \mathrm{d}\theta' \tag{8}$$

which is a continuous version of the matrix equation (5). The propagator $G(\Delta\theta, \Delta\tau)$ which is analogous to the matrix A in (6) is the probability distribution the additional turn $\Delta\theta$. We have assumed that G does not depend on τ. This results from the self-similarity of DLA which implies that the flux line encounters statistically similar structures and turns similarly at various levels of side-branching.

Equation (8) can be studied similarly to (5). Since $G(\Delta\theta) = G(-\Delta\theta)$, the propagator admits the cosine expansion:

$$G(\Delta\theta) = \frac{1}{2\pi} + \sum_{n=1}^{\infty} \frac{G_n}{\pi} \cos(n\Delta\theta)\,. \tag{9}$$

Using the expansion, the solution of the convolution equation (8) is found to be precisely the numerical findings for the distribution of the angle of attachment summarized in (2) and (3) with

$$\gamma_n = -\ln G_n / \Delta\tau\,. \tag{10}$$

The power-law decay of the amplitude with respect to N in (3) is an exponential decay with respect to $\tau = \ln N$ which is proportional to the number of branch orders in the cluster as explained above. This is analogous to the exponential decay of the amplitude with respect to the number of generations l in (7) for the Koch curve. We expect that the propagator is a smooth function. Therefore, G_n decreases quickly with n and explains why the decay rate γ_n is much larger for higher harmonics.

5. Propagation of walker flux lines

We have already suggested an explanation for the power-law decay of the amplitudes in the cosine expansion of the distribution of the angle of attachment. However, calculating theoretically the decay exponents γ_n requires knowledge of the propagator G. Any direct numerical determination of G to verify (10) requires computation of the flux lines for very large clusters, which is well beyond the capability of conventional methods [2]. Alternatively, we can gain some insight by examining simple plausible forms of G.

We first consider the simplest case that every turn $\Delta\theta$ is much smaller than π so that G is in the form of a narrow peak. For τ larger than $\Delta\tau$, equation (8) reduces to the diffusion equation:

$$\frac{\partial}{\partial\tau}P(\theta,\tau) = \nu\frac{\partial^2}{\partial\theta^2}P(\theta,\tau) \tag{11}$$

where ν is the diffusion coefficient depending on the width of G. The diffusion equation gives $\gamma_n = \nu n^2$, implying that $\gamma_2/\gamma_1 = 4$. This value has the correct order but is significantly different from the numerical value 6.7(3) [3].

We also tried Gaussian forms of G with larger width. However, the resulting values of γ_2/γ_1 are only slightly bigger than 4. We then consider the next simplest form of a modified Gaussian:

$$G(\Delta\theta) \sim \exp[-(\Delta\theta/\theta_0)^4] \tag{12}$$

and finally we are able to match the numerical value of γ_2/γ_1. By also matching both γ_1 and γ_2 computed from (10) simultaneously with the numerical values from Lam *et al* [3] summarized in section 2, we obtain $\theta_0 \simeq 94^\circ$ and $\Delta\tau \simeq \ln 130$. A plausible propagator in the form of (12) is thus determined. From equation (12), the average magnitude of a turn is $\langle|\Delta\theta|\rangle \simeq 0.49\theta_0 \simeq 46^\circ$. It means that a flux line typically turns through an additional angle of about $\pm 46^\circ$ whenever N increases by a factor of $\exp(\Delta\tau) \simeq 130$. For a cluster of size $N = 10^6$, each flux line has on average $N_t \simeq \ln N/\Delta\tau \simeq 2.8$ turns. We also tried a very different form of G which is the sum of two Gaussians:

$$G(\Delta\theta) \sim \exp\left[-\frac{(\Delta\theta-\theta_1)^2}{2\sigma^2}\right] + \exp\left[-\frac{(\Delta\theta+\theta_1)^2}{2\sigma^2}\right]. \tag{13}$$

The result is quite insensitive to the value of σ provided it is in a reasonable range such as 5° to 30° and we take $\sigma = 10^\circ$. Matching γ_1 and γ_2 similarly gives $\langle|\Delta\theta|\rangle \simeq \theta_1 \simeq 41^\circ$ and the number of turns $N_t \simeq 4.0$. There are infinitely many other possible functional forms of G which are consistent with the numerical values of γ_1 and γ_2 and we have no means to discriminate them.

The average magnitude of the turns $\langle|\Delta\theta|\rangle$ is dictated by the branch structure and should be roughly equal to the angle subtended between the side branches and the parent branches. It is quite interesting that the two simple choices of trial propagator give sensible values of $\langle|\Delta\theta|\rangle \simeq 46$ and 41 obtained above, since they are not far from Ossadnik's result on the branch subtending angle which is 38°.

The average number of turns N_t in a flux line was estimated above to be about 2.8 or 4.0 respectively, for the two trial propagators for a million particle cluster. Recall that N_t equals approximately the number of levels of side branches a flux line encounters when it extends from infinitely to the cluster. The maximum branch order in a cluster of a million particles was found to be approximately 10 by Ossadnik [7]. However, most flux lines terminate at the outer regions of the cluster so that they encounter only a very limited number of levels. As a result, N_t should be much smaller than 10. It seems that $N_t \simeq 3$ or 4 are reasonable estimates.

6. Self-similarity of walker flux lines

Visual examination of the flux lines in figure 1 indicates that they are in general smooth curves. However, they bend more and more frequently at regions closer and closer to the cluster. We suggest that due to the self-similarity of DLA every individual walker flux line obeys some type of scaling for length scales between those of an individual particle and the cluster. We emphasize that the self-similarity concerned is only restricted to segments of the flux line containing the point of contact of the line with the cluster. Specifically, a segment

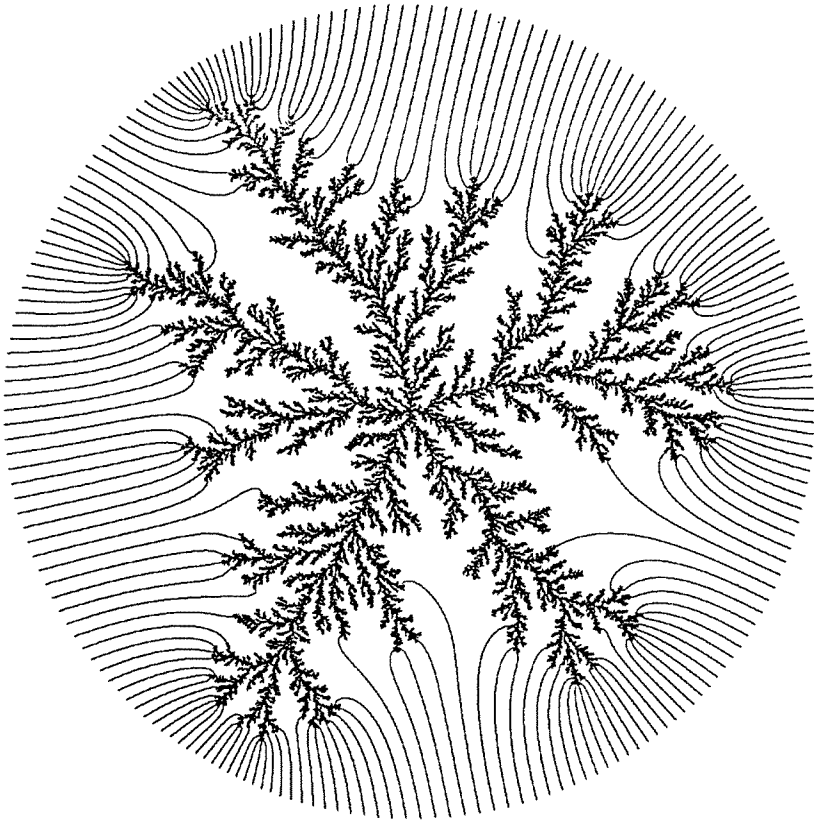

Figure 1. Example of 200 particle probability flux lines with uniformly spaced starting position on a circle of radius $4R_G$, where R_G is the radius of gyration of the above one million particle DLA cluster. The potential was solved by an over-relaxation method in a circular region of radius $4R_G$ on a grid with lattice spacing $8R_G/7000$. The displayed region has radius $2R_G$.

of a flux line which contains the point of contact and has a length much shorter than the radius of the cluster but much larger than that of the walkers is self-similar. Assume that we partition it further into two pieces. The partition which contains the point of contact is a random curve which is statistically similar to the original segment after proper rescaling back to the origin length. This type of self-similarity is similar to that of a spiral. A segment of a spiral containing the centre resembles the original spiral after proper magnification. However, an arbitrary segment of a spiral can simply be an arc, for example, and is not necessarily similar to the original spiral.

The motivation for the above self-similarity of the flux lines is as follows. As explained in section 4, while a flux line extends from infinity to the cluster, it bends whenever it encounters a deeper level of side-branching. We have explained that there is an additional turn whenever the cluster size increases by a factor of $\exp(\Delta\tau)$ so that the radius of the cluster increases by a factor of $r = \exp(\Delta\tau)^{1/D}$, where $D \simeq 1.72$ is the fractal dimension of DLA. Whenever the flux line starts to be affected by a higher level of side-branching as it extends towards the cluster, it encounters similar structures but scaled down by a factor of r due to the self-similar hypothesis of DLA. Let l be the length of the segment of the flux line between the ith and the $(i+1)$th turn. The length of the segment between the $(i+1)$th and the $(i+2)$th turn is thus l/r.

We can now construct a very simple model to highlight the self-similar geometry of the flux lines at length scales in between that of the cluster and the walkers. We start from the region further away from the cluster with a straight line of length l_0. To extend it to regions closer to the cluster, we join it end-to-end to another line segment of length l_0/r. The angle subtended between the two line segments is a random variable θ sampled from a trial propagator such as the modified Gaussian distribution in (12) with parameters specified in section 5. Then $r = \exp(\Delta\tau)^{1/D} \simeq 17$ where $\Delta\tau = \ln 130$, obtained in section 5, is used. We can similarly join further segments to the model flux line. The ith segment has length $l_0/r^{(i-1)}$ and subtends an independent random angle sampled from (12) with the $(i-1)$th segment. Since the scale factor $r = 17$ is indeed quite large, after adding a few segments, the curve converges quickly to a point representing the point of contact of the flux line with the cluster. Such a model flux line, after proper smoothing, is expected to have statistical properties approximating those of real flux lines.

7. Discussions

We have suggested a theoretical description of the branch structure and the geometry of the walker flux lines in DLA to describe the numerical results on the probability distribution of the branch orientation and the angle of attachment. In particular, the cosine probability distribution for the angle of attachment and the power-law decay of its amplitude with respect to the cluster size are reproduced by a simple convolution equation. Both extrapolations from the numerical results of Lam *et al* [3] and our present arguments support asymptotic local isotropy of DLA. They are consistent with the hypothesis that the local structure of DLA is non-directed. As far as isotropy is concerned, DLA is more similar to the Koch curve than the directed recursive model [9]. We also suggest that every single flux line is self-similar.

As pointed out in [3], available DLA clusters are strongly anisotropic and the approach to isotropy for increasing cluster size is extremely slow. The anisotropy decreases when there are more levels of side-branching in the cluster. The slow convergence to isotropy is because there are only about 10 levels of side-branching even in a cluster of a million particles [7]. Moreover, section 5 explained that only about 3 or 4 of them are close enough to the outer regions of the cluster to be contacted by flux lines of considerable weight and

be relevant to the growth. In addition, the angle subtended between branches is only about 38° [7]. The small angle also leads to inefficient randomization of the orientations of the branches and contributes to the extremely slow crossover.

Since the magnitude of the local anisotropy depends on the number of levels of side-branching in the cluster, for DLA in radial geometry, when the number of levels increases by adding more particles, the anisotropy diminishes. For the case of cylindrical geometry, or diffusion-limited deposition, investigated numerically by Hegger and Grassberger [6], at the early stage of deposition, the amplitude of the distribution of the angle of attachment decays similarly with respect to the cluster size with an exponent α. Due to a different relationship between the total number of branch levels and the cluster size in this configuration, α is different from our exponent γ_1 and is given by $\alpha = \gamma_1 D/(D-1)$ where D is the fractal dimension of DLA. Their numerical value of α is in good agreement with Lam *et al*'s γ_1 [3] as expected from the hypothesis that the local properties of DLA is independent of the overall boundary conditions. When the height of the cluster is comparable to the width for the case of deposition, the number of levels of branching ceases to increase further and the anisotropy should converge to a finite magnitude instead of vanishing as for DLA. Hegger *et al* also measured the orientation of the last step of a walker before sticking. From simple geometrical argument, this angle differs from the angle of attachment by a random additive term of small magnitude. Therefore, all the statistics are similar.

The conclusion of asymptotic local isotropy contradicts the claim of self-affinity based on Meakin and Vicsek's density correlation measurements [4] mentioned in section 1. We expect that this is due to strong finite-size effects in their measurements. Let $C_R(r)$ be the correlation between two points separated by a distance r in a cluster of radius R. If $1 \ll r \ll R$ is well satisfied using much bigger clusters, isotropy in the scaling of the correlation function may be achieved. In contrast, the self-affinity hypothesis requires the scaling to be anisotropic, in particular, in this regime since Meakin and Vicsek's investigation covers both the cases $r \ll R$ and $r \sim R$. The condition $1 \ll r$ is necessary to avoid discretization effects so that scaling in the correlation function can be possible. On the other hand, $r \ll R$ corresponds to locality and is a necessary condition for isotropy. This condition is necessary even for the simple Koch curve to reveal its locally isotropic property as explained in section 3. In view of the slow approach to local isotropy, observing the convergence of the radial and tangential decay exponent of the density correlation is extremely difficult. In addition, the correlation measurement is actually not quite suitable for isotropy testing because it does not discriminate the radially outward and inward directions while the attachment probabilities in these two directions happen to be most different.

There are other numerical results which lead to conclusion of local anisotropy of DLA [9]. Detailed investigation of these methods is beyond the scope of this paper. However, due to the extremely slow convergence to local isotropy, the apparent local anisotropy may result from finite-size effects. Finite-size effects in various measurements of DLA have been discussed recently [10].

Laplacian growth can be formulated by complex analytical methods by defining a conformal map $f(z)$ from the unit disc in the complex plane to the region outside the cluster [11]. The angle of attachment is precisely the argument of $f'(z)$ evaluated at an appropriate point on the unit circle. It can be shown that the convolution equation (8) implies interesting properties of the coefficients in the power series expansion of $f'(z)$. However, we have not been able to obtain further physical predictions in this scheme.

References

[1] Witten T A and Sander L M 1981 *Phys. Rev. Lett.* **47** 1400; 1983 *Phys. Rev.* B **27** 2586
[2] Vicsek T 1992 *Fractal Growth Phenomena* 2nd edn (Singapore: World Scientific)
[3] Lam C H, Kaufman H and Mandelbrot B B 1995 *J. Phys. A: Math. Gen.* **28** L213
[4] Meakin P and Viscek T 1985 *Phys. Rev.* A **32** 685
[5] Mandelbrot B B and Viscek T 1989 *J. Phys. A: Math. Gen.* **22** L377
[6] R Hegger and P Grassberger 1994 *Phys. Rev. Lett.* **73** 1672
[7] Ossadnik P 1992 *Phys. Rev.* A **45** 1058
[8] Feder J, Hinrichsen E L, Måløy K J and Jøssang T 1989 *Physica* **38D** 104
[9] Mandelbrot B B, Kaufman H, Vespignani A, Yekutieli I and Lam C H 1995 *Euro. Phys. Lett.* **29** 599
[10] Lam C H 1995 *Phys. Rev.* E **52** 2841
[11] See for example: Bensimon D, Kadanoff L P, Liang S, Shraiman B I and Tang C 1986 *Rev. Mod. Phys.* **58** 977